

Unified description of LHC data on elastic pp scattering

Yu.M. Shabelski and A.G. Shuvaev

Petersburg Nuclear Physics Institute, Kurchatov National Research Center
Gatchina, St. Petersburg 188300, Russia

E-mail: shabelsk@thd.pnpi.spb.ru

E-mail: shuvaev@thd.pnpi.spb.ru

Abstract

We present the unified description of the existing data on elastic small angle pp and $p\bar{p}$ scattering at the energies 1.8, 1.96, 2.76, 7, 8 and 13 TeV in the framework of Additive Quark Model. The agreement with the data is quite reasonable.

1 Introduction

In the previous papers [1–3] we describe the differential cross section of elastic pp scattering at $\sqrt{s} = 7$ TeV. The real part of pp elastic amplitude measured at $\sqrt{s} = 13$ TeV has been described in [4]. Recently the new data on elastic scattering cross section $d\sigma/dt$ became available at the energies 2.76, 8 and 13 TeV. In the present paper we show that these data can be reasonable described in the same manner after a little modification of the internal parameters.

Our approach is based on the Additive Quark Model (AQM). In AQM baryon is treated as a system of three spatially separated compact objects – the constituent quarks. Each constituent quark is colored and has an internal quark-gluon structure and a finite radius that is much less than the radius of the proton, $r_q^2 \ll r_p^2$. The constituent quarks play the roles of incident particles in terms of which pp scattering is described. Elastic amplitudes for large energy $s = (p_1 + p_2)^2$ and small momentum transfer t are dominated by Pomeron exchange. We neglect the small difference in pp and $p\bar{p}$ scattering coming from the exchange of negative signature Reggeons such as the Odderon (see e.g. [5] and references therein), ω -Reggeon etc., since their contributions are suppressed by s . The single t -channel exchange results into the amplitude of

constituent quarks scattering,

$$A_{qq}^{(1)}(s, t) = \gamma_{qq}(t) \cdot \left(\frac{s}{s_0}\right)^{\alpha_P(t)-1} \cdot \eta_P(t), \quad (1)$$

where $\alpha_P(t) = \alpha_P(0) + \alpha'_P \cdot t$ is the Pomeron trajectory specified by the intercept $\alpha_P(0)$ and the slope value α'_P . The Pomeron signature factor,

$$\eta_P(t) = i - \tan^{-1} \left(\frac{\pi \alpha_P(t)}{2} \right),$$

determines the complex structure of the amplitude. The factor $\gamma_{qq}(t) = g_1(t) \cdot g_2(t)$ has the meaning of the Pomeron coupling to the beam and target particles, the functions $g_{1,2}(t)$ being the vertices of the constituent quark-Pomeron interaction. In the following we assume the Pomeron trajectory to have the simplest form,

$$\left(\frac{s}{s_0}\right)^{\alpha_P(t)-1} = e^{\Delta \cdot \xi} e^{-r_q^2 q^2}, \quad \xi \equiv \ln \frac{s}{s_0}, \quad r_q^2 \equiv \alpha'_P \cdot \xi.$$

The value r_q defines the radius of the quark-quark interaction, while $S_0 = (9 \text{ GeV})^2$ has the meaning of typical energy scale in Regge theory. The scattering amplitude is presented in AQM as a sum over the terms with a given number of Pomerons,

$$A_{pp}(s, t) = \sum_n A_{pp}^{(n)}(s, t), \quad (2)$$

where the amplitudes $A_{pp}^{(n)}$ collect all the diagrams comprising various interactions between the beam and target quarks going through n Pomerons exchange. Similar to Glauber theory [6, 7] the multiple interactions between the same quark pair has to be ruled out. AQM permits the Pomeron to connect any two quark only once. It crucially decreases the combinatorics, leaving the diagrams with no more than $n = 9$ effective Pomerons.

The Pomeron connects to the proton through the form factor,

$$F_P(Q_1, Q_2, Q_3) = \int dk_i \psi^*(k_1, k_2, k_3) \psi(k_1 + Q_1, k_2 + Q_2, k_3 + Q_3). \quad (3)$$

Here $\psi(k_1, k_2, k_3)$ is the initial proton wave function written in terms of the constituent quarks' transverse momenta k_i , $\psi(k_1 + Q_1, k_2 + Q_2, k_3 + Q_3)$ is the wavefunction of the scattered proton. A more detailed description can be found in Ref. [1]. The quarks' wave function has been taken in the simple form of Gaussian packets,

$$\psi(k_1, k_2, k_3) = N [e^{-a_1(k_1^2 + k_2^2 + k_3^2)} + C_1 e^{-a_2(k_1^2 + k_2^2 + k_3^2)} + C_2 e^{-a_3(k_1^2 + k_2^2 + k_3^2)}], \quad (4)$$

normalized to unity,

$$\int |\psi(k_1, k_2, k_3)|^2 \delta^{(2)}(k_1 + k_2 + k_3) d^2 k_1 d^2 k_2 d^2 k_3 = 1.$$

2 Comparison with the data

The results of our calculations are presented for the relatively small t . The large t values are beyond the validity of AQM since it treats the constituent quarks as point like particles without an internal structure. Differential cross section $d\sigma/dt$ are shown in Fig.1 (left) together with the experimental data for $\sqrt{s} = 13$ TeV. The model provides fairly well fit to the data for $|t| < 0.6$ GeV². The results for $\sqrt{s} = 8$ TeV are shown in Fig.1 (right). Unfortunately the experimental data are available at this energy not up to the dip position.

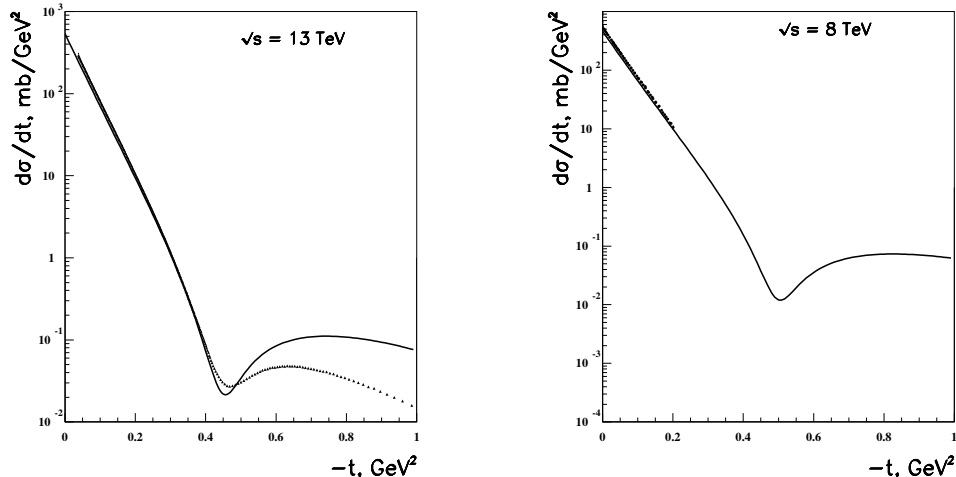


Figure 1: The differential cross section of elastic pp scattering at $\sqrt{s} = 13$ TeV (left) and $\sqrt{s} = 8$ TeV (right). The experimental points have been taken from [10–13].

The calculated ratio of the real to imaginary part of the elastic scattering amplitude at $t = 0$ is $\rho = 0.82$ for $\sqrt{s} = 13$ TeV. It agrees with the experimental value 0.9 ± 0.01 [8] while being only a little bit smaller than the other value, 0.10 ± 0.01 , reported in the same Ref. [8].

Fig.2 presents $d\sigma/dt$ data for $\sqrt{s} = 7$ TeV and $\sqrt{s} = 2.76$ TeV. The calculations for 7 TeV yield an appropriate fit to the data though the output total cross section $\sigma_{tot} = 93.1$ mb is smaller than the experimental estimation 98.6 ± 2.2 mb [9]. The position of the minimum obtained at 2.76 TeV is slightly righter than the experimental

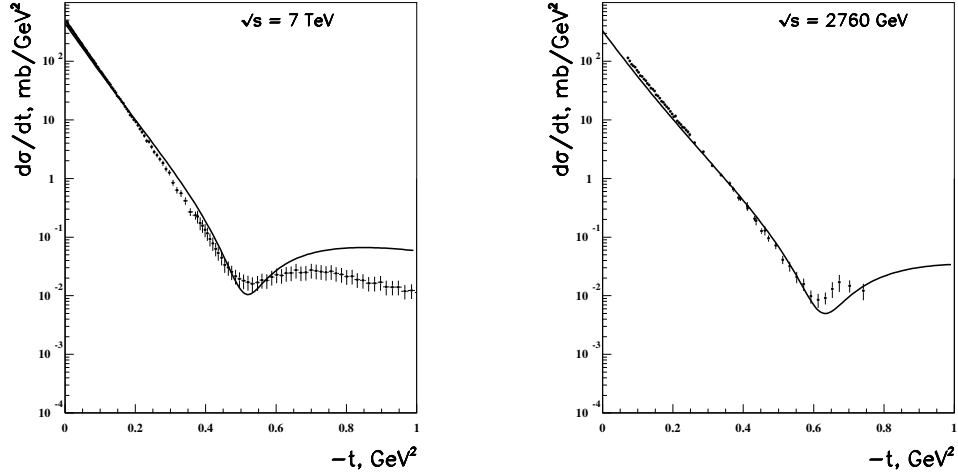


Figure 2: The differential cross section of elastic pp scattering at $\sqrt{s} = 7$ TeV (left) and $\sqrt{s} = 2.76$ TeV (right). The experimental points have been taken from [9, 14, 15] .

one. It is important to note that the values of the total cross section, slope of the diffractive cone and the location of the minima of the differential cross section are strongly correlated at the each energy.

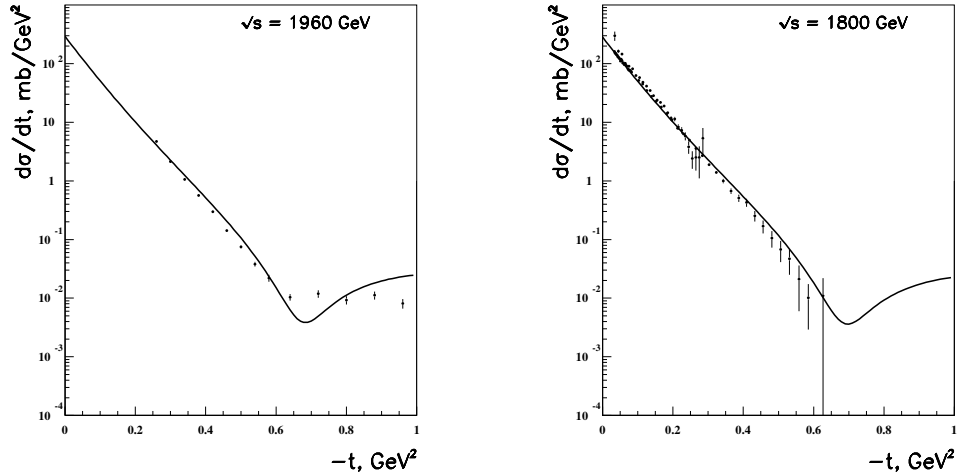


Figure 3: The differential cross section of elastic $p\bar{p}$ scattering at $\sqrt{s} = 1.96$ TeV (left) and $\sqrt{s} = 1.8$ TeV (right). The experimental points have been taken from [16–19].

To better illustrate applicability of the model we also present what it gives for the $p\bar{p}$ elastic scattering at the lower energies. The comparison with the FNAL data at the energies 1.96 TeV and 1.8 TeV, Fig.3, exhibits a quite acceptable description, however the dip at 1.96 TeV is again right of its experimental position.

All model curves have been obtained with the following set of parameters:

$$\Delta = 0.139, \quad \alpha' = 0.122 \text{ GeV}^{-2}, \quad \gamma_{qq} = 0.49 \text{ GeV}^{-2}. \quad (5)$$

$$a_1 = 8.0 \text{ GeV}^{-2}, \quad a_2 = 0.255 \text{ GeV}^{-2}, \quad a_3 = 1.45 \text{ GeV}^{-2}, \quad C_1 = 0.026, \quad C_2 = 0.054.$$

The calculated total cross section, slope of the diffractive cone B ($d\sigma/dt = A \exp(-B|t|)$) and the ratio of the real to imaginary part of the elastic pp (or $\bar{p}p$) amplitude, $\rho = \text{Re } A/\text{Im } A$, are compared with the existing experimental data in the Table.

\sqrt{s}	σ_{tot} (mb)	B (GeV^{-2}) (mb/GeV^2)	$\text{Re } A/\text{Im } A$ ($t = 0$)
13 TeV	102.4	20.4	0.082
[10]	110.5 ± 2.4		
[11]		$20.40 \pm 0.002 \pm 0.01$	
[8]			0.09 ± 0.01
[8]			0.10 ± 0.01
8 TeV	95.1	19.6	0.083
[12]	101.5 ± 2.1		
[12]	101.9 ± 2.1		
[13]	102.0 ± 2.3		0.12 ± 0.03
[13]	103.0 ± 2.3		
7 TeV	93.1	19.4	0.083
[14]		$23.6 \pm 0.5 \pm 0.4$	
[9]	98.6 ± 2.2	19.9 ± 0.3	
2.76 TeV	80.0	18.0	0.087
[15]		17.1 ± 0.3	
1.96 TeV	75.5	17.5	0.089
[16]		$16.86 \pm 0.1 \pm 0.2$	
1.8 TeV	74.4	17.4	0.089
[17]		16.99 ± 0.47	
[18]			0.14 ± 0.069

3 Discussion and conclusion

As is seen from the Table the calculated cross sections are smaller than the experimental ones at the LHC energies. The output σ_{tot} values can be increased by readjusting the model parameters, but it moves the diffractive dip to the left and causes the growth

of the ρ ratio. Given the fact that the experimental dip position is directly measured whereas an additional analysis is needed to get the absolute normalization of the cross section, we prefer to chose the above listed parameters (5). Despite some mismatch in the experimental slopes B of the diffractive cones at small t the general trend of its energy dependence is properly reproduced.

To summarize, the conventional AQM with a rather simple set of parameters results in quite reasonable description of the small angle hard scattering. Though we are unable to exclude completely effects from the Odderon exchange [15] their contribution seems not to be significant. Here we agree with Ref. [20].

The authors are grateful to M.G. Ryskin for helpful discussion.

References

- [1] Y. M. Shabelski and A. G. Shuvaev, JHEP **1411** (2014) 023 [arXiv:1406.1421 [hep-ph]].
- [2] Y. M. Shabelski and A. G. Shuvaev, Eur. Phys. J. C **75** (2015) 9, 438 [arXiv:1504.03499 [hep-ph]].
- [3] Y. M. Shabelski and A. G. Shuvaev, Eur. Phys. J. C **76** (2016) no.8, 470 [arXiv:1601.04426 [hep-ph]].
- [4] Y. M. Shabelski and A. G. Shuvaev, Eur. Phys. J. C **78** (2018) no.6, 497 [arXiv:1802.02812 [hep-ph]].
- [5] R. Avila, P. Gauron and B. Nicolescu, Eur. Phys. J. C **49**, 581 (2007) [hep-ph/0607089].
- [6] R. J. Glauber. In "Lectures in Theoretical Physics", Eds. W. E. Brittin et al., New York (1959), vol.1, p.315.
- [7] V. Franco and R. J. Glauber, Phys.Rev. **142** (1966) 1195.
- [8] G. Antchev *et al.* [TOTEM Collaboration], arXiv:1812.04732 [hep-ex].
- [9] TOTEM Collaboration, G. Antchev et al., Europhys.Lett. **101** (2013) 21002.
- [10] G. Antchev *et al.* [TOTEM Collaboration], Eur. Phys. J. C **79** (2019) no.2, 103 [arXiv:1712.06153 [hep-ex]].

- [11] G. Antchev *et al.* [TOTEM Collaboration], arXiv:1812.08283 [hep-ex].
- [12] G. Antchev *et al.* [TOTEM Collaboration], Nucl. Phys. B **899** (2015) 527 [arXiv:1503.08111 [hep-ex]].
- [13] G. Antchev *et al.* [TOTEM Collaboration], Eur. Phys. J. C **76** (2016) no.12, 661 [arXiv:1610.00603 [nucl-ex]].
- [14] TOTEM Collaboration, G. Antchev *et al.*, Europhys.Lett. **95** (2011) 41001, [arXiv:1110.1385].
- [15] G. Antchev *et al.* [TOTEM Collaboration], arXiv:1812.08610 [hep-ex].
- [16] V. M. Abazov *et al.* [D0 Collaboration], Phys. Rev. D **86** (2012) 012009 [arXiv:1206.0687 [hep-ex]].
- [17] N. A. Amos *et al.* [E-710 Collaboration], Phys. Lett. B **247** (1990) 127.
- [18] N. A. Amos *et al.* [E710 Collaboration], Phys. Rev. Lett. **68** (1992) 2433.
- [19] F. Abe *et al.* [CDF Collaboration], Phys. Rev. D **50** (1994) 5518.
- [20] V. A. Khoze, A. D. Martin and M. G. Ryskin, Phys. Lett. B **784** (2018) 192 [arXiv:1806.05970 [hep-ph]].